International Soil and Water Conservation Research 11 (2023) 112–124

Contents lists available at ScienceDirect

International Soil and Water Conservation Research

journal homepage: www.elsevier.com/locate/iswcr

Original Research Article

Quantification and depth distribution analysis of carbon to nitrogen ratio in forest soils using reflectance spectroscopy

Asa Gholizadeh [a, *], Mohammadmehdi Saberioon [b], Nastaran Pouladi [a, c], Eyal Ben-Dor [d]

[a] Department of Soil Science and Soil Protection, Faculty of Agrobiology, Food and Natural Resources, Czech University of Life Sciences Prague, 16500, Prague, Czech Republic
[b] Section 1.4 Remote Sensing and Geoinformatics, Helmholtz Centre Potsdam GFZ German Research Centre for Geosciences, Telegrafenberg, 14473, Potsdam, Germany
[c] knoell Germany GmbH, Konrad-Zuse-Ring, 68163, Mannheim, Germany
[d] Remote Sensing Laboratory, Department of Geography and Human Environment, Porter School of Environment and Earth Science, Tel Aviv University, 69978, Tel Aviv, Israel

ARTICLE INFO

Article history:
Received 10 March 2022
Received in revised form
23 May 2022
Accepted 22 June 2022
Available online 31 July 2022

Keywords:
Forest soil
Soil organic carbon
C:N
Soil horizons
VNIR–SWIR spectroscopy

ABSTRACT

Forest soils have large contents of carbon (C) and total nitrogen (TN), which have significant spatial variability laterally across landscapes and vertically with depth due to decomposition, erosion and leaching. Therefore, the ratio of C to TN contents (C:N), a crucial indicator of soil quality and health, is also different depending on soil horizon. These attributes can cost-effectively and rapidly be estimated using visible–near infrared–shortwave infrared (VNIR–SWIR) spectroscopy. Nevertheless, the effect of different soil layers, particularly over large scales of highly heterogeneous forest soils, on the performance of the technique has rarely been attempted. This study evaluated the potential of VNIR–SWIR spectroscopy in quantification and variability analysis of C:N in soils from different organic and mineral layers of forested sites of the Czech Republic. At each site, we collected samples from the litter (L), fragmented (F) and humus (H) organic layers, and from the A_1 (depth of 2–10 cm) and A_2 (depth of 10–40 cm) mineral layers providing a total of 2505 samples. Support vector machine regression (SVMR) was used to train the prediction models of the selected attributes at each individual soil layer and the merged layer (profile). We further produced the spatial distribution maps of C:N as the target attribute at each soil layer. Results showed that the prediction accuracy based on the profile spectral data was adequate for all attributes. Moreover, F was the most accurately predicted layer, regardless of the soil attribute. C:N models and maps in the organic layers performed well although in mineral layers, models were poor and maps were reliable only in areas with low and moderate C:N. On the other hand, the study indicated that reflectance spectra could efficiently predict and map organic layers of the forested sites. Although, in mineral layers, high values of C:N ($\geq$ 50) were not detectable in the map created based on the reflectance spectra. In general, the study suggests that VNIR–SWIR spectroscopy has the feasibility of modelling and mapping C:N in soil organic horizons based on national spectral data in the forests of the Czech Republic.

1. Introduction

Soil organic carbon (SOC) is the largest terrestrial carbon (C) pool in the biosphere (Lal, 2008) and plays a key role in mitigating global atmospheric carbon dioxide (CO_2) level. SOC has several significant functions in the environment (Murphy, 2014) such as maintaining soil structure and physical stability (Ayoubi et al., 2020). Accordingly, it is crucial to a number of natural processes linked to soil health and fertility (Dinakaran et al., 2016). Soil total nitrogen (TN) is also one of the important indicators of the ecological environment and part of the organic matter components

* Corresponding author.
E-mail addresses: gholizadeh@af.czu.cz (A. Gholizadeh), saberioon@gfz-potsdam.de (M. Saberioon), npouladi@knoell.com (N. Pouladi), bendor@tauex.tau.ac.il (E. Ben-Dor).

https://doi.org/10.1016/j.iswcr.2022.06.004

and mineralization process in soil (Li et al., 2014; Shang et al., 2014). These attributes affect the supply of food, air, fresh water and agritourism and even associate to the sustainable development of the local economy (Keesstra et al., 2012; Zhang et al., 2007). They have also been used as proxies to assess soil quality and land degradation in some Himalayan and Mediterranean areas (Kukal & Bawa, 2014; Munoz-Rojas et al., 2015).

Forest soils contain a large amount of the world's SOC, TN and energy resources. They influence the quality and composition of the atmosphere and form climate conditions on different scales (Baciak et al., 2015). In forest ecosystems, SOC and TN cycles are related via a number of fundamental processes including litterfall, primary production, mineralization of organic matter components and decomposition rate (Albrechtova et al., 2008). The ratio of SOC to TN (hereafter C:N) in soil, particularly in forest soil, is another important indicator of soil fertility and quality reflecting the interaction or coupling between SOC and TN (Lou et al., 2012; Xu et al., 2018), which is considered as a proxy of C sequestration potential in soils (Akselsson et al., 2005; Vries et al., 2006). Soil C:N also delivers information about the decomposition stage of soil organic matter that is known as an essential factor of soil fertility, and hence highlights the microorganism activities in soil. High values of C:N (>40) demonstrate the availability of fresh organic matter, whereas lower values (around 5–15) indicate partially to fully decomposed organic matter (Nolan et al., 2011). Therefore, the level of C:N in forest soils is one of the important predictors for estimating soil functions such as C storage capacity of soil and biomass production. When integrated into risk assessment, these functions can serve for modelling scenarios of soil sustainability with climate change issues (Carre et al., 2010). The abovementioned issues highlight that quantifying the concentration and spatial distribution of SOC, TN and specifically their ratio (C:N) are useful for evaluating and improving forest soil management, ecological environment monitoring and climate policy establishment.

The concentrations of SOC, TN and consequently C:N level in forest ecosystem are different depending not only on geographic location but also on soil horizon (Brahma et al., 2018; Lal, 2008) due to different stages of decomposition, erosion and leaching (Black et al., 2014; Gibson et al., 2002). For instance, the decreasing trend of SOC concentration with depth in different forested sites of China and the Czech Republic were reported (Gholizadeh et al., 2021; Jia et al., 2017) and linked to the reduction of below-ground plant biomass with soil depth that as a result has a considerable effect on C:N vertical alteration. Moreover, C:N vertical changes can also happen in response to TN leaching (Cools et al., 2014). Lal (2017) stated that there need to be much attention in the storage of SOC in the top 40 cm of soil. Zanella et al. (2017) categorized this depth into organic and mineral horizons. Accordingly, since these soil layers noticeably contribute to concentrations of SOC, TN and thus C:N level, particularly in forested areas, the vertical quantification and variability analysis of them should be taken into account.

The number of observations and soil variability to a great extent influence on soil attributes determination at large-scale (e.g., regional and national) studies (Bellamy et al., 2005; Chamberlain et al., 2010). Nevertheless, the cost and efficiency connected to soil sampling, laboratory analysis and assessment of SOC, TN and therefore C:N in organic and mineral horizons of forest soils using conventional analytical techniques limit their large-scale prediction due to the requirement of a large number of samples (Chen et al., 2019; Vanguelova et al., 2016), particularly if the aim is measurement of depth (England & Viscarra Rossel, 2018). Quick, cost-effective and reliable approaches for effective determination of SOC, TN and C:N in forest soil horizons are thus essential.

Visible–near infrared–shortwave infrared (VNIR–SWIR) spectroscopy is an efficient technique to rapidly and accurately predict soil attributes over large areas at depth, while reducing the cost of soil sampling and analysis (Ben-Dor & Banin, 1995; Gholizadeh et al., 2013; Naimi et al., 2022). The spectral data acquired from VNIR–SWIR spectroscopy can then sufficiently characterize the spatial (vertical and lateral) as well as the temporal variability of soil (Viscarra Rossel et al., 2017). The technique has been successfully used to measure SOC and TN concentrations at different scales (Barthes et al., 2006; Gholizadeh et al., 2011, 2018; Knadel et al., 2012; Viscarra Rossel & Hicks, 2015). There are also a few local-scale studies investigating the use of reflectance spectroscopy for assessing forest SOC in different horizons (Wang et al., 2019; Zhao et al., 2019). Developing large-scale (e.g., national, continental and global) spectral-based model though may be an approach to enhance the success of the technique (Viscarra Rossel et al., 2016). Gholizadeh et al. (2021) used VNIR–SWIR spectroscopy to predict and characterize SOC in different horizons of forest soils over the Czech Republic; however, so far, the capability of VNIR–SWIR spectroscopy for large-scale prediction and spatial analysis of C:N in forest soil layers has not yet fully been exploited.

In this context, the current study attempts to overcome this lacuna and foster VNIR–SWIR reflectance spectroscopy to quantify the levels of SOC, TN and C:N in forest soil organic and mineral horizons. In addition, as there is a lack of information on the depth distribution of C:N at the national scale in the Czech Republic, the study aims to evaluate the efficiency of VNIR–SWIR spectroscopy to examine the spatial distribution of C:N in different forest soil layers of the whole country. The premise of this study is that there is a large heterogeneity in the vertical spatial distribution of soil C:N in the forested areas of the country. As VNIR–SWIR spectroscopy can cover large sampling points, both horizontally and vertically, it is also anticipated that the technique can provide massive SOC, TN and thus C:N data, which can facilitate to get a general overview on quality of forest soils in Central Europe.

2. Materials and methods

2.1. Study sites, soil sampling and laboratory analysis

One-third of the Czech Republic land (78,865 km^2) is covered by forests (Czech Statistical Office for Surveying, Mapping and Cadastre, 2019). The sampling sites of the current study were distributed over all the country's forested sites (Fig. 1).

The samples used in this study were originally from the Forest Soil Survey (Fiala et al., 2013). During the years 2000–2008, the samples were collected from the forested areas of the whole country. Five-hundred and one (501) samples were separately

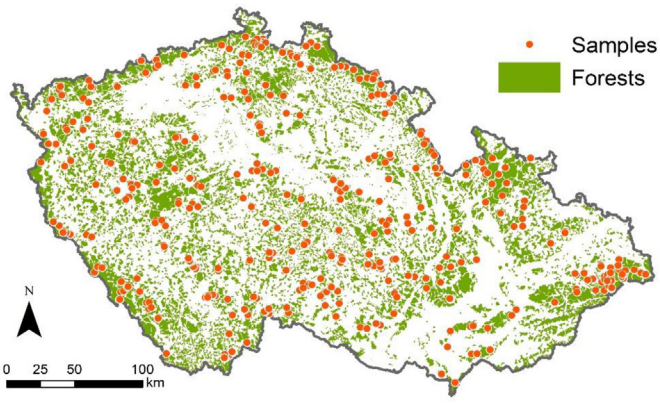

Fig. 1. Locations of the forests and soil sampling sites in the Czech Republic.

obtained from three individual organic horizons of litter (L), fragmented (F), humus (H), as well as the mineral horizon of A_1 (with thickness usually from 2 to 10 cm) and the subsurface mineral horizon of A_2 (typically to the depth of 40 cm) to build a dataset of consisting 2505 samples. The position of each sampling point was recorded using a GeoXM (Trimble Inc., Sunnyvale, CA, USA) receiver with an accuracy of 1 m.

Before any analysis, the soil samples were gone through common preparation procedure (air-dried, finely ground, sieved to $\leq$ 2 mm) and thoroughly mixed (ISO11464:2006). SOC was measured as total oxidized C using wet oxidation (Sparks, 1996) and TN was determined by the Kjeldahl digestion distillation method (Bremner & Mulvaney, 1982). The histograms of SOC, TN and C:N in different layers can be seen in Fig. 2. Since TN and C:N in the mineral layers (A_1 and A_2) didn't meet the requirements of a normal distribution, the log transformation of their values was carried out to drastically reduce the skewness and obtain reliable predictions.

2.2. Spectroscopic measurements

Spectral reflectance was recorded across the 350–2500 nm wavelength range using an ASD FieldSpec III Pro FR spectroradiometer (ASD Inc., Denver, Colorado, USA) with a high-intensity contact probe. Fig. 3 indicates the scanning setup for the samples' measurement in this study.

The spectral resolution of the spectroradiometer was 2 nm for the region of 350–1050 nm and 10 nm for the region of 1050–2500 nm. In addition, the radiometer bandwidth from 350 to 1000 nm was 1.4 nm while it was 2 nm from 1000 to 2500 nm. Based on our laboratory's protocol, the instrument ran for about 30 min to warm up the spectrometer and lamp before any measurement. To avoid beam reflectance from the bottom of the dish (Jensen, 2007), the soil samples were placed in 9 cm diameter Petri dishes and formed 2 cm layers of soil. According to Mouazen et al. (2005), a smooth soil surface guarantees maximum light reflection and a high signal to noise ratio (SNR). Thus, to generate a flat surface with the top of the Petri dish, the samples were leveled off and spectral scanning was made in three replications (in the center of each sample) in a dark room and the average was saved. The spectroradiometer was optimized using a white Spectralon™ (Labsphere, North Sutton, New Hampshire, USA) before the first scan and after every six measurements (Shi et al., 2016).

2.3. Data preprocessing and spectral modelling

All spectra, per soil layer, were preprocessed before modelling. First, we removed the noisy portions between 350 and 400 nm, as well as 2451 and 2500 nm, spectra in the range from 400 to 2450 nm (2051 variables) were kept for further processing. The spectral reflectance (R) was transformed into apparent absorbance spectra through log 10(1/R) and the spectra were then subjected to Savitzky-Golay smoothing (Savitzky & Golay, 1964) with a second-order polynomial fit and 11 smoothing points in order to remove the artificial noise within the working spectral range. The first derivative was afterwards generated and used to remove baseline offset and enhance spectral features (Gholizadeh et al., 2013). Because of high collinearity of the spectra and to reduce dimensionality, 0.1 nm resolution was extracted from whole spectra and we retained only every tenth wavelength from 400 to 2450 nm (Gholizadeh et al., 2021). It is also necessary to analytically detect reference data outliers in the datasets (Martens & Naes, 1992). The histograms of data, from all soil layers, were therefore plotted and distribution and normality of data were checked. Afterwards, the outliers were identified and eliminated, both visually and employing the principle of the Cook distance. This outlier detection technique is applied in regression analysis to detect influential outliers in a set of predictor variables (Cook, 1977; Kim, 2017). The number of removed outliers was 73, 70, 53, 23 and 57 for layers L, F, H, A_1 and A_2, respectively. The principal component analysis (PCA) was also performed and the scoreplot of the first two principal components (PCs) was used to visualize the structure of the data (Dotto et al., 2018) and to highlight the soil variations in different horizons with different C:N levels.

To build prediction models that given a spectrum will be able to predict either SOC, TN and C:N, the data from each soil layer (L, F, H, A_1 and A_2) as well as the dataset obtained from merging all individual layers (profile) were randomly split into training (75%) and testing (25%) datasets using the Kennard Stone (KS) technique (Kennard & Stone, 1969). To develop the regression models and to validate the developed models' generalization capability, the training sets and the testing sets were used, respectively (Kooistra et al., 2003). The spectral modelling was performed using support vector machine regression (SVMR) algorithm with radial basis kernel. The algorithm follows supervised learning based on the statistical learning theory (Vohland et al., 2011). It has been identified to strike the correct balance between the accuracy gained from a given limited amount of training patterns and the generalization capability to handle unseen data (Kovacevic et al., 2009). It should be noted that a basic grid search approach was applied to tune SVMR's hyperparameters (i.e., cost function and sigma). The implementation of SVMR for spectroscopic modelling has previously been described in detail by Viscarra Rossel and Behrens (2010) and Gholizadeh et al. (2016). The spectroscopic models were finally validated using 10-repeated 10-fold cross-validation (Hastie et al., 2009) and the validation statistics provided here are the means of the 10 repeats. The entire spectra preprocessing and modelling procedures were done using the software R 4.1.0 (R Development Core Team, Vienna, Austria).

2.4. Prediction performance assessment

The final performance of the models was assessed using standard model evaluation statistics: the coefficient of determination (R^2) values between the observed and predicted values of SOC, TN and C:N, Lin's concordance correlation coefficient (LCCC), root mean squared error (RMSE) and bias. R^2 (Eq. (1)) is the proportion of variation in the response that can be described by the regression model and shows the precision of the relationships. RMSE (Eq. (2)) is usually used in VNIR–SWIR spectroscopy to explain the prediction capability of a model and bias (Eq. (3)) is an independent metric that represents the error of means (Bellon-Maurel et al., 2010; Gomez et al., 2016), which both indicate the accuracy of the prediction models (Ghebleh et al., 2021). LCCC (Eq. (4)) is a single index that ranges between 0 and 1 (the larger the value, the better the fitting effects) and evaluates the precision and accuracy of the model (Lin, 1989).

$$R^2 = \frac{\sum_{i=1}^{n}(predicted_i - \overline{observed})^2}{\sum_{i=1}^{n}(observed_i - \overline{observed})^2} \quad (1)$$

$$LCCC = \frac{2r\sigma_{observed}\sigma_{predicted}}{\sigma^2_{observed} + \sigma^2_{predicted} + (\overline{predicted} - \overline{observed})^2} \quad (2)$$

$$RMSE = \sqrt{\frac{1}{n}\sum_{i=1}^{n}(observed_i - predicted_i)^2} \quad (3)$$

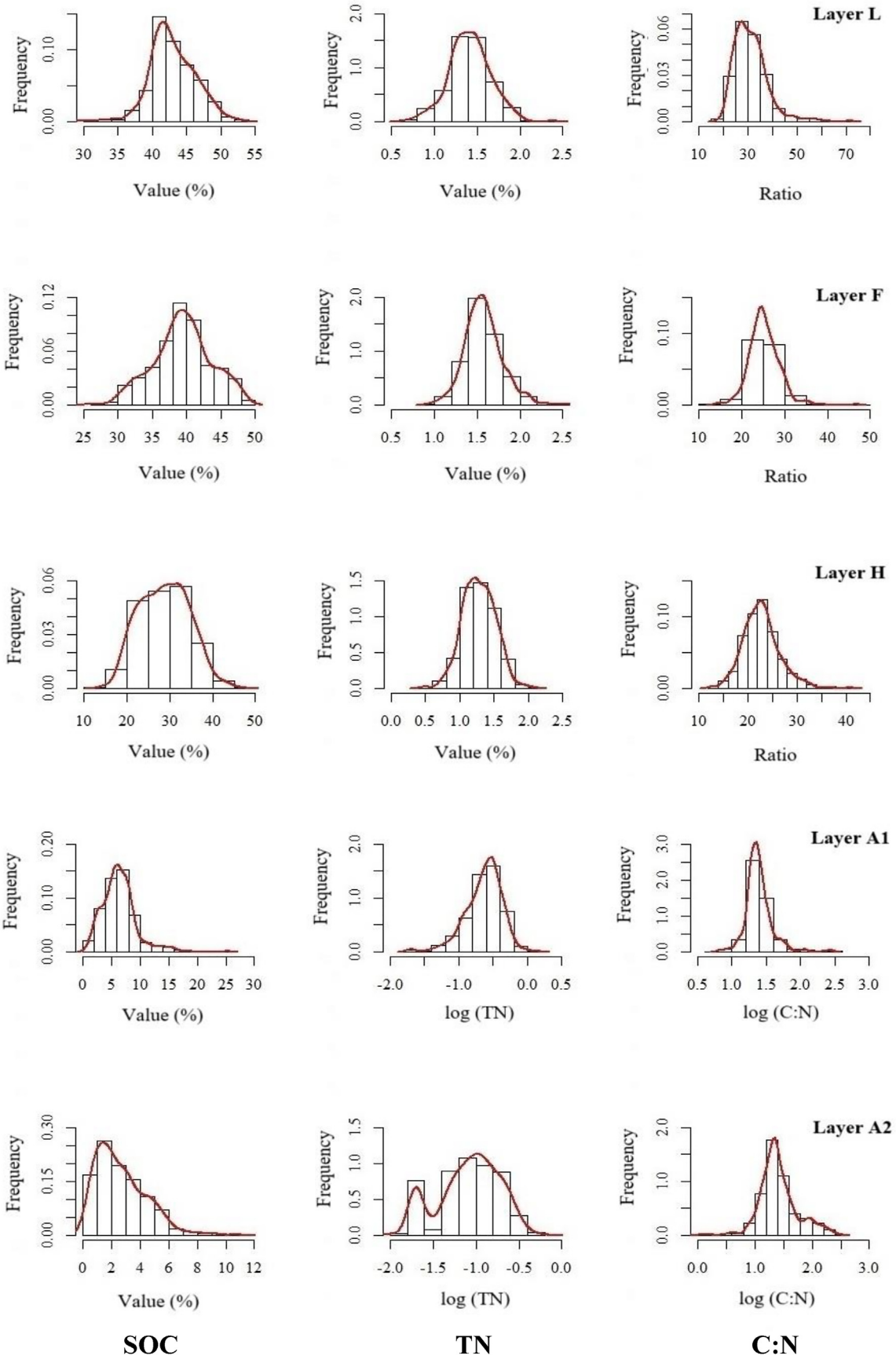

Fig. 2. Histograms of SOC, TN and C:N for each soil layer.

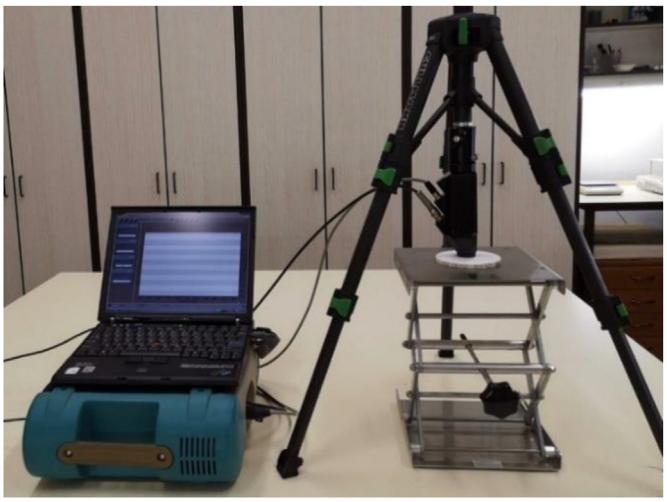

Fig. 3. Spectra measurement setup.

$$bias = \frac{1}{n}\sum_{i=1}^{n}(observed_i - predicted_i) \quad (4)$$

where $predicted_i$ and $observed_i$ are the predicted and observed values at the time i; n is the number of total samples; $\overline{predicted}$ and $\overline{observed}$ are the mean values of the predicted and observed soil attribute; r is the Pearson correlation coefficient between the predicted and observed soil attribute; $\sigma_{predicted}$ and $\sigma_{observed}$ are the standard deviations of predicted and observed soil attribute.

2.5. Spatial distribution of C:N

The spatial distribution of C:N in different forest soil layers acquired through chemical analysis and lab spectroscopy, was then mapped as follows:

i) semi-variograms were created to estimate the spatial correlations and the appropriate variogram models.
ii) spatial distribution maps of C:N were obtained using an ordinary kriging method.

Afterwards, the resulting maps were compared to evaluate the capability of prediction models to determine the depth spatial distribution of C:N. The mapping procedure was conducted in the R 4.1.0 software (R Development Core Team, Vienna, Austria).

3. Results

3.1. Preliminary findings of soil attributes at different layers

General statistical results of SOC, TN and C:N including minimum, maximum, mean, standard deviation (Std.), coefficient of variation (CV) and skewness from all sampling locations for the profile and the individual layers (L, H, F, A_1 and A_2) are shown in Table 1.

Different layers were remarkably different in terms of SOC contents, and a large variation in SOC content in soils of the profile as well as the individual layers was seen, which is linked to the different depths from which the soil was sampled. The SOC mean in the L layer was very high (mean = 43.08% ± 2.93% (Std.)) ranged from 36.67% to 50.91%. These contents decreased to mean = 39.46% ± 4.12% and 28.80% ± 5.60% in layers F and H and ranges = 29.50–48.79% and 15.10–42.84%, respectively. In the mineral layers A_1 and A_2, the average SOC contents were noticeably lower (5.96% and 2.65%) than the organic layers (L, F and H) with minimum and maximum of 0.82% and 12.20% for A_1 and 0.18% and 10.70% for A_2. Almost a similar trend can be observed in average of TN contents, declining with the depth, except in layer F (mean = 1.58% ± 0.20%), which showed the highest TN contents among all layers (even more than L with mean = 1.44% ± 0.20%). The TN contents were low in mineral layers, particularly in A_2 with minimum and mean values of 0.01% and 0.12%, respectively.

Table 1
Statistics description of soil attributes for profile and the individual horizons.

Layer	N	Minimum	Maximum	Mean	Std.	CV (%)	Skewness
SOC (%)							
L	426	36.67	50.91	43.08	2.93	7	0.47
F	431	29.50	48.79	39.46	4.12	10	−0.05
H	446	15.10	42.84	28.80	5.60	19	0.06
A_1	476	0.82	12.20	5.96	2.29	39	0.02
A_2	444	0.18	10.70	2.65	1.76	67	1.01
Profile	2223	0.18	50.91	23.29	17.05	73	−0.08
TN (%)							
L	426	0.97	2.01	1.44	0.20	14	0.29
F	431	1.03	2.11	1.58	0.20	13	0.27
H	446	0.69	1.86	1.28	0.22	18	0
A_1	476	0.03	0.55	0.25	0.11	45	0.37
A_2	444	0.01	0.54	0.12	0.08	70	1.28
Profile	2223	0.01	2.11	0.91	0.65	71	−0.15
C:N							
L	426	21.07	47.16	30.54	5.15	17	0.39
F	431	17.69	33.92	25.19	2.90	12	0.08
H	446	14.98	32.10	22.66	3.29	15	0.30
A_1	476	6.16	111.60	26.23	12.20	47	2.84
A_2	444	1.13	112.00	28.83	21.00	73	2.02
Profile	2223	1.13	112.00	26.55	11.77	44	3.43

L: litter; F: fragmented; H: humus; N: number of samples; Std.: standard deviation; CV: coefficient of variation.

In terms of C:N, the similar pattern of reducing C:N by increasing depth was not followed despite the trend were seen for SOC and TN contents. Table 1 indicates that the average C:N in the L layer was higher than all the other individual layers, presenting a high mean value of 30.54 ± 5.15, while layer H showed the lowest C:N mean of 22.66 ± 3.29. In addition, there were higher C:N contents in the mineral layers of A_1 and A_2 (mean = 26.23 and 28.83, respectively) compared to the organic layers of F and H. A comparison of the studied layers' CVs highlights that layer A_2 had the highest variation of C:N (CV = 73%), which shows that its distribution is the most heterogeneous among all soil layers. The very wide range of C:N in this layer (1.13–112.00) caused lack of homogeneity in the population, probably due to the availability of SOC in different decomposition stages. In contrast, layer F had the CV = 12%, considered as low variability. The data with CV > 35%, 15% < CV < 35% and CV < 15% values has been classified as high, moderate and low variability, respectively (Wilding, 1985). The C:N data for all layers positively skewed with the highest skewness of 2.84 in A_1. The individual organic layer of F had approximated a normal distribution (skewness = 0.08), whereas layers L and H were mildly skewed. The whole profile results highlight that the average C:N of all samples was 26.55% ± 11.77%, with a distribution that shows rather a moderate variability (CV = 44%) and a highly and positively skewed distribution (skewness = 3.43).

3.2. Soil spectral information at different layers

PCA was applied on the VNIR–SWIR spectra of the forest soil

samples from different organic and mineral layers with different concentrations of SOC and TN. As shown in Fig. 4 and mentioned in section 2.3., some samples were scattered away from the majority of the samples and therefore were considered as outliers. The first two PCs demonstrated about 98.63% variation and the organic layers (L, F and H) spectra were obviously separated from the mineral layers (A_1 and A_2) spectra; however, a spectral similarity was observed between the layers in each group of spectra (Fig. 4). This can be related to changes in concentrations and types of the studied soil attributes by depth (Table 1), particularly due to SOC decomposition process (Gholizadeh et al., 2021). The findings of the PCA scoreplot justify the need to investigate the effect of different soil layers on C:N ratio using VNIR–SWIR spectroscopy. It also demonstrates the power of PCA to discriminate VNIR–SWIR reflectance spectra of soils from different depths.

Fig. 5 presents the average reflectance of soil samples from different layers (L, H, F, A_1 and A_2) and their standard deviation. Average raw spectra shapes and patterns for all soil layers, regardless of the depth, were typical for soil reflectance, with a steady increase through VIS wave range (400–700 nm) and sharp absorption bands, particularly in the SWIR range (1900–2500 nm). The organic layers of L, F and H obviously followed a progression associated with reduction in their organic matter contents; however, the spectra of layer H showed remarkably lower mean reflectance values. Furthermore, the soil samples of the A_1 layer also indicated lower albedo intensity and reflectance across the entire spectra than other the L, F and A_2 layers. Nevertheless, they had wider variance compared to layers L and F. In addition, it can be seen in Fig. 5 that the spectra for the forest soil samples collected from the A_2 layer were typical of soils with lower SOC concentration, with common absorptions due to iron oxides, water and clay minerals, mainly in NIR and SWIR regions.

3.3. SOC and TN prediction model performance at different soil layers

The results of the SOC and TN estimation models at different forest soil layers according to their R^2, LCCC, RMSE and bias values are presented in Table 2.

For SOC prediction, the differences between individual layers' models in case of R^2 were somehow negligible ($0.63 \leq R^2 \leq 0.77$). Layer H showed the lowest $R^2 = 0.63$ and also the highest RMSE and bias values (RMSE = 3.56% and bias = −0.49%) among all individual layers in estimation of SOC, while F performed the best prediction

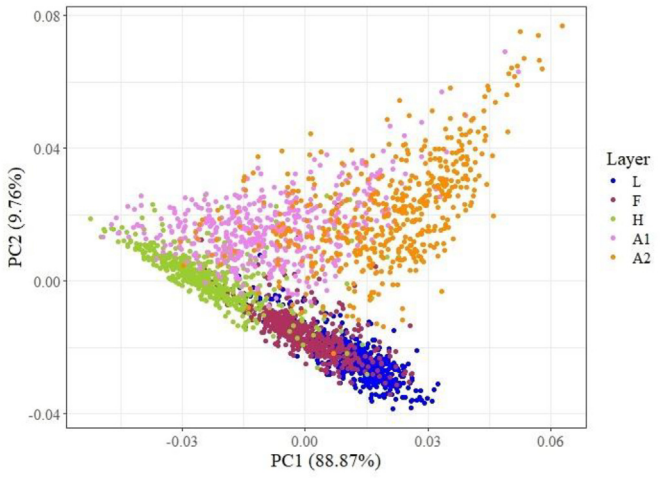

Fig. 4. PCA for VNIR–SWIR spectra applied on different soil layers.

results with the highest R^2 and lowest RMES and bias (low-biased spatial estimates) values (R^2 = 0.77, RMSE = 1.72% and bias = −0.05%). In addition, layer F had LCCC = 0.85, which is higher than other layers and shows the best 1:1 fit. The prediction accuracies obtained for assessing TN in the individual soil layers in terms of R^2 were noticeably lower ($0.45 \leq R^2 \leq 0.71$) than those gained for SOC. But similarly, they showed the same trend as SOC, where the F layer (R^2 = 0.71, LCCC = 0.85, RMSE = 0.07% and bias = 0%), performed better than the other layers and especially than H (R^2 = 0.45, LCCC = 0.63, RMSE = 0.18% and bias = 0.02%). The most significant finding about TN prediction in all examined layers (either individual or merged) was that they were almost unbiased ($-0.01\% \leq$ bias $\leq 0.02\%$). Furthermore, for both SOC and TN, the models developed for the organic horizons of L and F were more accurate than those of the mineral horizons of A_1 and A_2.

Table 2 also highlights that for both assessed attributes (SOC and TN), the best prediction accuracies with high R^2 and LCCC and low RMSE values were obtained, when all layers (profile) were used for development of the models (R^2 = 0.97 and 0.95, LCCC = 0.99 and 0.98, RMSE = 1.68% and 0.06%, respectively). Moreover, the profile models for both attributes showed low error (bias), although the profile model of TN was unbiased (bias = 0).

3.4. C:N quantification and spatial distribution at different soil layers

Assessment metrics in Table 3 show the performance of the SVMR models, when predicting C:N in profile and the individual layers. It can be seen that the difference in C:N prediction accuracy between the organic and mineral layers was more considerable than their SOC and TN separately. In other words, the assessment metrics obtained for the organic layers in general, and for the L and F data in particular (R^2 = 0.69 and 0.71, LCCC = 0.81 and 0.84, RMSE = 2.72% and 2.17% and bias = 0.37% and −0.23%), were noticeably better than of the mineral layers of A_1 and A_2 particular (R^2 = 0.32 and 0.31, LCCC = 0.48 and 0.44, RMSE = 7.66% and 9.52% and bias = 0.85% and 1.26%).

According to Table 3, the R^2 and LCCC (0.71 and 0.84) were higher for layer F than other forest soil layers. Likewise, in prediction of samples collected from the layer F, RMSE and bias showed the lowest values (2.17% and −0.23%, respectively) among all examined layers. This was similar to SOC and TN prediction results presented in Table 2. The scatterplots of the observed against predicted C:N for each soil layer support these results (Fig. 6). Table 3 and Fig. 6 also show that merging all individual soil layers, we obtained the soil profile prediction model, which could fairly (Chang et al., 2001) perform (R^2 = 0.63, LCCC = 0.79, RMSE = 7.48% and bias = 0.46%). The profile model was more accurate than the model for the individual layers of H, A_1 and A_2; nonetheless, less accurate than layers L and F models.

When the models were validated, the next step was the spatial prediction of C:N in different soil layers using the observed data obtained from wet chemistry and the predicted data derived from VNIR–SWIR spectra. Fig. 7 highlights the resulting depth distribution maps, which reflect important information of the soil C:N condition.

It could be observed that the spatial distribution of soil C:N across the forested sites of the country was similar across all soil layers, typically decreasing from west to east. It was also noticed that generally, VNIR–SWIR spectroscopy could fairly predict and spatially analyze C:N in the organic horizons (L, F and H) of the forested sites of the Czech Republic. In these layers, the same tendency and a coherent spatial distribution were clearly observed between the observed and predicted maps. Even layer H, with lower accuracy compared to L and F, highlighted the different

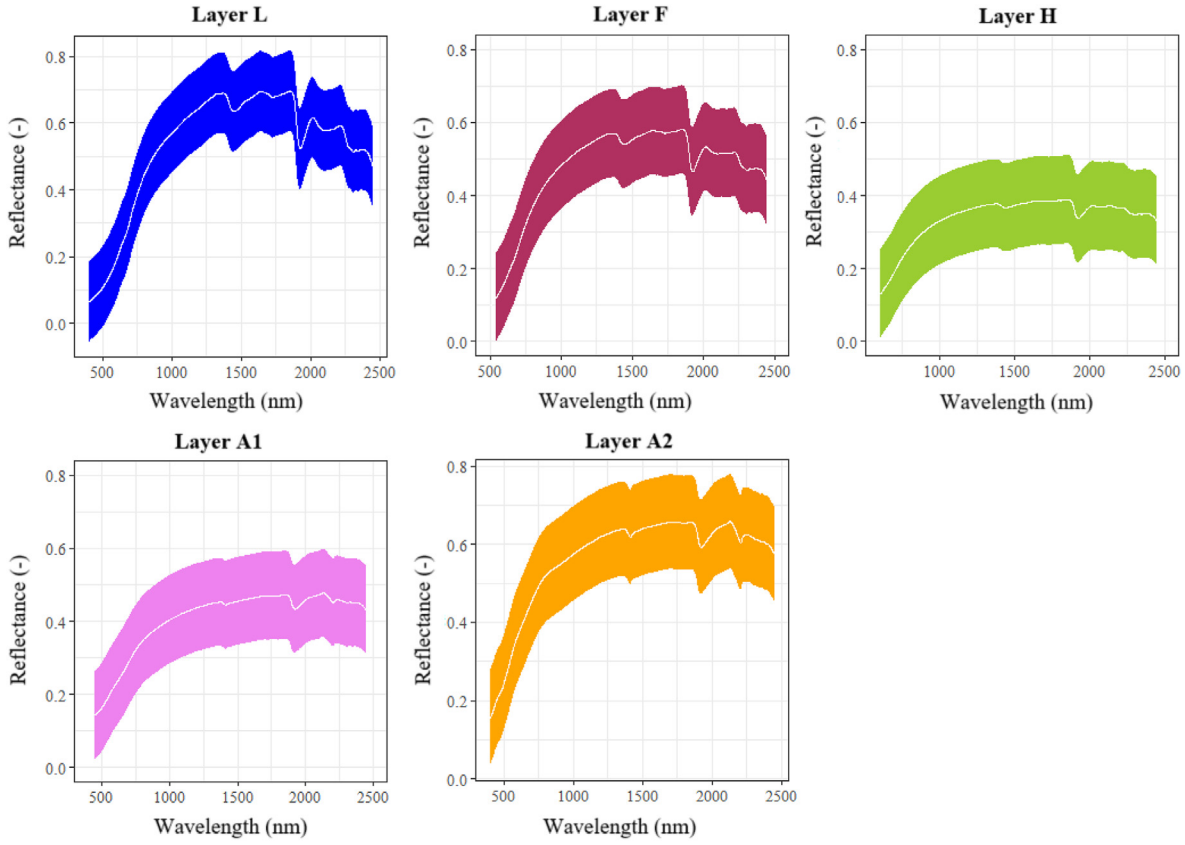

Fig. 5. Average reflectance spectra (bold line) and their variance (shaded area) of forest soil samples collected from different layers.

Table 2
SOC and TN prediction model performance at profile and different soil layers.

Layer	N	R^2	LCCC	RMSE	bias
SOC					
L	426	0.74	0.82	1.75	0.10
F	431	0.77	0.85	1.72	−0.05
H	446	0.63	0.74	3.56	−0.49
A_1	476	0.65	0.74	2.03	0.39
A_2	444	0.71	0.76	1.87	0.38
Profile	2223	0.97	0.99	1.68	0.21
TN					
L	426	0.62	0.70	0.09	−0.01
F	431	0.71	0.73	0.07	0
H	446	0.45	0.63	0.18	0.02
A_1	476	0.55	0.66	0.14	0.01
A_2	444	0.60	0.69	0.13	0.01
Profile	2223	0.95	0.98	0.06	0

L: litter; F: fragmented; H: humus; N: number of samples; R^2: coefficient of determination; LCCC: Lin's concordance correlation coefficient; RMSE: root mean square error.

values of C:N.

This trend did not work thoroughly well for the mineral layers. For instance, regarding layer A_1, in the easternmost part of the study area, where the lowest values concentrated, a similar spatial trend could be seen between the observed and predicted maps. However, towards the west, C:N pattern and values were quite variable between the maps, without a clearly distinguishable spatial pattern and without depicting the C:N values higher than 50 (Fig. 7). The least accurate spatial variability map was for the A_2 layer as the deepest studied layer. It can be seen that similar to layer

Table 3
C:N prediction model performance at profile and different soil layers.

Layer	N	R^2	LCCC	RMSE	bias
C:N					
L	426	0.69	0.81	2.72	0.37
F	431	0.71	0.84	2.17	−0.23
H	446	0.56	0.66	4.28	0.48
A_1	476	0.32	0.48	7.66	0.85
A_2	444	0.31	0.44	9.52	1.26
Profile	2223	0.63	0.79	7.48	0.46

L: litter; F: fragmented; H: humus; N: number of samples; R^2: coefficient of determination; LCCC: Lin's concordance correlation coefficient; RMSE: root mean square error.

A_1, high values of C:N (≥ 50) were not detectable in the map created based on the reflectance spectra and the largest section of the study area was covered with the low and moderate values with no significant spatial variability. It can be mentioned that, in the mineral layers (A_1 and A_2), VNIR–SWIR reflectance spectra were efficient only to map lower values of C:N with highly degraded SOC. In general, findings in Fig. 7 highlighted that VNIR–SWIR spectroscopy could detect different classes of C:N in the organic layers, especially L and F, but it failed to differentiate various classes of C:N in forest mineral layers. These results are in agreement with those of presented in Table 3 and Fig. 6.

4. Discussion

According to Table 1, the forest soils of the Czech Republic had high SOC concentration in general with the profile mean concentration of 23.29%. In terms of soil layers, the organic layer of L

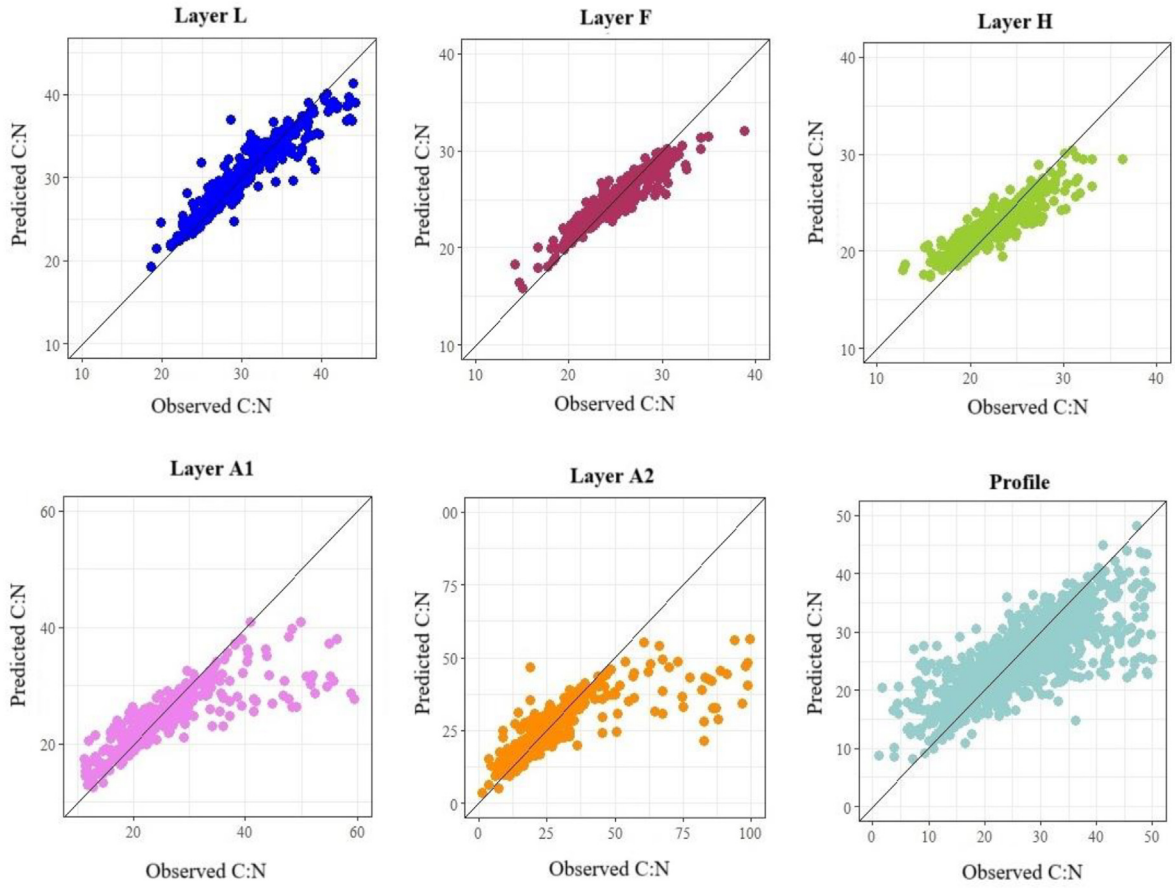

Fig. 6. Scatterplots of the observed against predicted C:N at different soil layers.

showed the highest SOC (mean = 43.08%), which decreased with increasing soil depth. This trend was proved in previous studies (Gelaw et al., 2013; Gholizadeh et al., 2021; Ugawa et al., 2012; Zhang et al., 2016). This is attributed to the litter serving as the main source of forest SOC. The organic composition of litter is gradually decomposed by microorganisms, hence enriching the top soils (Jiang et al., 2017). Moreover, SOC decrease by depth is due to the increasing intensity of microbially-driven decomposition (Kramer et al., 2017). In addition, the most dominant soil class of the Czech Republic and this study's sample set was Cambisols, in which there is little C below the organic horizons. These soils do not show any significant soil development with depth, although they have thick organic rich surface horizons (Deluca & Boisvenue, 2012). In this study, TN mirrored the SOC concentrations trend (Table 1) and almost a similar trend was observed between TN and forest soil depth, which was also reported in the studies by Kramer et al. (2017) and Sorenson et al. (2020). This can be associated with the mineralization of litter from trees into fine particles and substances such as ammonium (NH_4^+) that usually sticks to the surface layers (Zhang et al., 2016).

With exception of layer H, all other layers had the values of C:N higher than 24, suggesting that the net nitrification was low (Ollinger et al., 2002; Albrechtova et al., 2008). Nevertheless, high C:N may also be indicative of nitrogen immobilization by nitrogen restricted soil microbial community (Holub et al., 2005). The organic horizons of L, F and H followed the decreasing trend of C:N, similar to what was observed for SOC and TN. Forest floor's (the L layer) C:N ranged from 21.07 to 47.16 (mean = 30.54), which was decreased by depth in the other organic layers (Table 1). This highlights the availability of more amount of fresh organic and less decomposed organic matter in this top layer (Carre et al., 2010). On the other hand, layer H, with the lowest value of C:N among others, represents well-decomposed organic matter and stable humus components. This is attributed to high accumulation of more extensively-decomposed (or microbially-altered) organic compounds in the lower layers after C loss to respiration (Jenkinson & Coleman, 2008; Krull & Skjemstad, 2003). In contrary, it was also clear in Table 1 that in the mineral horizons (A_1 and A_2), the average C:N increased as soil depth increased. This was opposite to the SOC and TN trends and the results obtained in a research by Kramer et al. (2017), who found soil C:N values were generally decreasing with increasing of soil depth. Whereas supported by the results yielded in some sites studied by Kramer et al. (2012), Zhang et al. (2016), Wehr et al. (2020) and Radocaj, Jurisic, and Antonic (2021). Working on Hawaiian soils, Kramer et al. (2012), found that organic matter resembling oxidized plant matter accumulated in the deeper soil horizons due to chemical association with short-range order minerals.

The scoreplot of PCA (Fig. 4) indicates the data compression and its dimensionality reduction. As expected, there was an obvious separation of data by soil layer (L, F, H, A_1 and A_2). It happened along the continuum of decomposition process and differences in concentrations of soil attributes (i.e., SOC and TN). Based on Fig. 4, spectral characteristics were consistent with variation in soil layers. Nevertheless, the obtained outputs were entirely different between organic and mineral layers, which may be linked to the variation in SOC concentrations of the samples that has a direct influence on spectral features and intensity (Ben-Dor & Banin, 1995). Moreover,

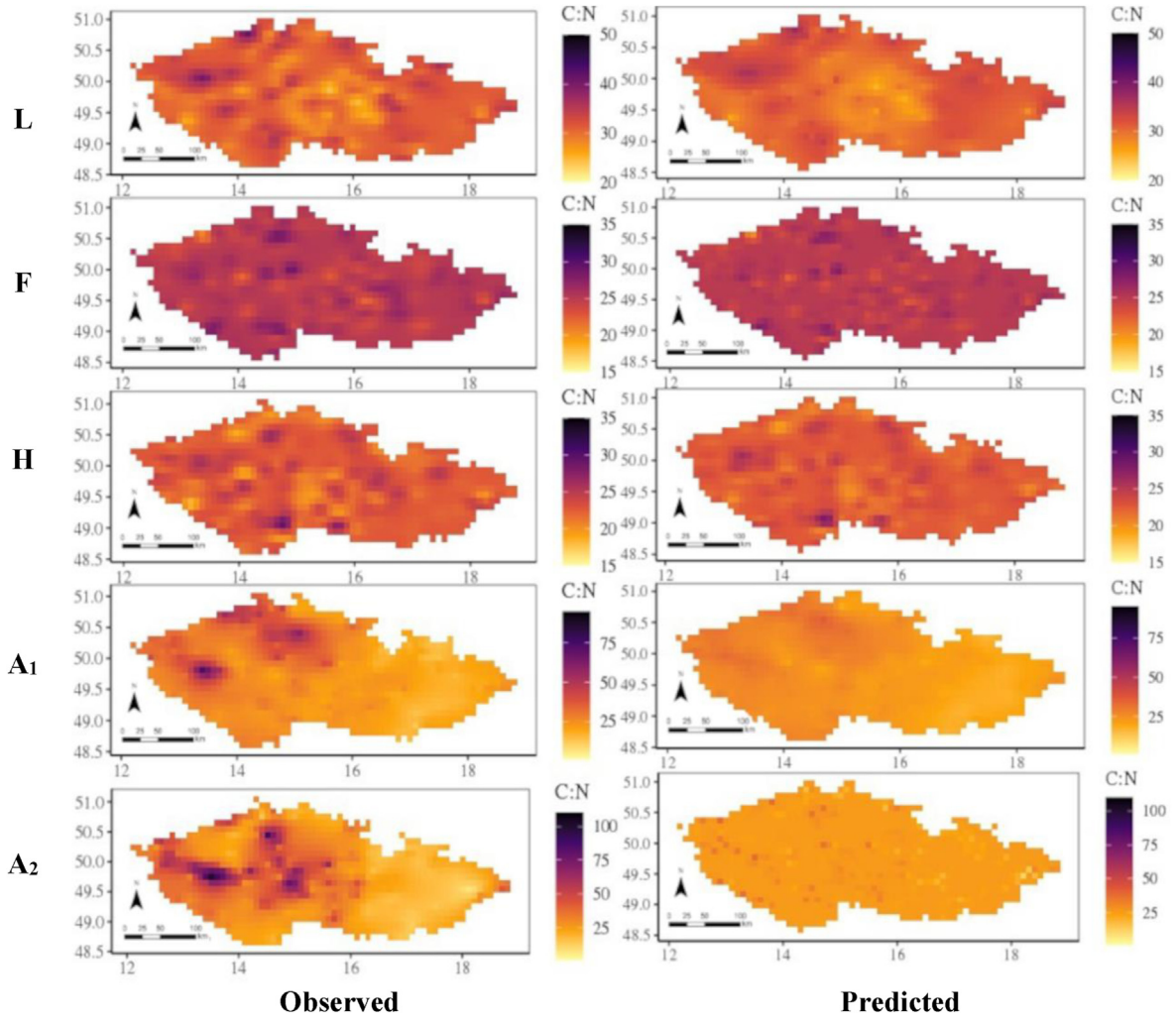

Fig. 7. Observed and predicted spatial distribution of C:N at different soil layers.

this can be expected due to significant differences in CV values of SOC, TN and C:N between organic and mineral layers (Table 1), which can cause wider scattering of samples in the mineral layers with higher CV values compared to the organic layers.

Fig. 5 highlights that the VNIR–SWIR spectra of all soil layers were similar in appearance with respect to pattern, but varied in reflectance values representing variation in TN and SOC concentrations and types (Sherman & Waite, 1985; Song et al., 2012). Kuang and Mouazen (2011) and Jia et al. (2014) stated that SOC and TN concentrations possess direct spectral response (overtone or combination) in the VNIR–SWIR region. For example, the bands around 1150 nm are attributed to the absorption of amine N–H and the variables near 2450 nm are related to the overtones of C–H bond in methyl (Viscarra Rossel & Behrens, 2010). In the current study, the main factors that dominated the spectral behavior of the soil horizons were probably the wide range of SOC concentrations (0.18%–50.91%) and types (e.g., recognizable fresh remains, humic component). This is consistent with the conclusions presented by Heil and Schmidhalter (2021). As the layers L and F contain less-decomposed organic matter (e.g., leaves, needles, little branches), their high spectral reflectance is largely caused by remained vegetation photosynthetic pigments (e.g., chlorophyll, carotenoids, xanthophylls) and cell structure (Gitelson et al., 2002). Layer H followed by A_1 indicated the lowest reflectance values compared to the other studied layers (Fig. 5), which is probably because of the darker colour of these layers and the well-decomposed structure laying at them (Zanella et al., 2017). However, the high reflectance of the A_2 layer can be associated with the very low contents of SOC and TN in this horizon (Table 1) that was also confirmed by Conforti et al. (2015) and Jia et al. (2017).

Prediction results in Table 2 indicate the ability of VNIR–SWIR spectra and the models to predict SOC and TN on a large scale was satisfactory in forest soils profile (merged individual layers). This may ascribe to strong correlation of SOC and TN with soil reflectance as often reported in the literature (Dinakaran et al., 2016; Peltre et al., 2011). The results also show that for both SOC and TN, statistics outputs were considerably higher, when all layers (profile) were used for model development. Such results are consistent with those described in studies by Xie et al. (2011) and Jia et al. (2017), in which the total samples from different depths generally provided better models than the surface and subsurface sets for the measurement of organic matter, SOC and TN concentrations, respectively. Kuang and Mouazen (2011) and Jia et al. (2017) mentioned that the heterogeneity and high CV of the sample sets could increase the accuracy of calibration models.

Considering SOC and TN prediction in individual horizons (Table 2), it was apparent that the L and F organic layers were predicted more accurately than the mineral layers of A_1 and A_2,

which is similar to the results obtained by Jia et al. (2017). It is probably because the spectral reflectance from the soil, as a predictor, becomes less efficient due to an acute decrease in the SOC and TN concentrations (Gholizadeh et al., 2021; Jia et al., 2017). Nevertheless, despite the decline in prediction capability with depth, the VNIR–SWIR spectra could still fairly assess the target attributes in deeper layers of the forested areas across the country. Furthermore, Table 2 indicates that layer F was the best-predicted horizon among the others, which can be associated with the contribution of TN and SOC type and their correlation with other soil attributes in this soil layer. This has also been reported in some other studies (Gholizadeh et al., 2018; Telles et al., 2003). In contrast, the H layer had the poorest prediction models of SOC and TN that can be linked to its very decomposed materials and high SD values (Table 1) among others (Jia et al., 2017; Kuang & Mouazen, 2011). In summary, these results revealed successful VNIR–SWIR models for SOC prediction (with high R^2 and LCCC and low error values) and moderate spectral models for TN prediction in different forest soil layers, though the TN developed models were low- or even zero-biased. These results compared well to previous literature (Ji et al., 2016; Jiang et al., 2017). It should be noted that the soil spectroscopic models established in local-scale studies usually perform better (Guerrero et al., 2016; Stevens et al., 2013), perhaps because the soils sampled at the local-scale have lower variability and more similar spectral features (Gholizadeh et al., 2021).

The findings in Table 3 and Fig. 6 explain that C:N prediction using VNIR–SWIR spectra was more accurate in the forest soil profile as well as organic horizons, particularly in the F layer, which is similar to those of obtained for SOC and TN individual assessment (Table 2). It is apparent from Table 3 that the developed models for the mineral horizons of A_1 and A_2 were poor and did not have reliable predictive ability. Mutuo et al. (2006) and Heil and Schmidhalter (2021) were either unable to accurately predict C:N in deeper layers in VNIR–SWIR studies. The very wide range of C:N in A_1 and A_2 layers (6.16–111.60 and 1.13–112.00, respectively) shows the availability of SOC in different decomposition stages, which has different spectral responses and generally causes a drop in model robustness and calibration accuracy due to lack of homogeneity in the population (Brunet et al., 2007; Dinakaran et al., 2016; Peltre et al., 2011). Contrarily, Jia et al. (2017) showed that the wide concentration range in soil attributes would be advantageous in developing satisfactory VNIR–SWIR spectroscopy models.

The observed and predicted data from wet chemistry and VNIR–SWIR reflectance spectroscopy were used to visualize the depth distribution of C:N in the country's forested sites (Fig. 7). The spatial distribution of soil C:N across the forests followed a rather comparable trend across all soil layers reducing from west to east. This might be connected to variation in forest stands (e.g., forest composition, soil classes and altitudes), which affect the SOC, TN and C:N dynamics of the forest soils (Albrechtova et al., 2008; Zhang et al., 2016), particularly in forest floor that is more easily influenced by external factors such as tree species (Ollinger et al., 2002; Zhang et al., 2016). In terms of depth effect, the maps of C:N created by the spectral data in the organic layers (particularly, layer F) generally showed similar spatial distribution patterns with those of obtained from the actual data. The predicted maps in these layers were capable of not only displaying low and medium C:N values, but also detecting high and very high classes of C:N. This can be attributed to rather fair to good prediction accuracy of C:N in organic layers (Table 3 and Fig. 6). In the target mineral layers (A_1 and A_2), differences in the range of C:N values occurred and high values were observed, which might be caused by soluble substances (such as NO_3^-) yielded from litters that are continuously taken into deep soil layers by infiltration (Zhang et al., 2016). However, in spite of the organic layers, VNIR–SWIR spectroscopy was not successful to classify high values of C:N in the mineral layers. This indicates that the effectiveness of C:N spectroscopic models in deeper forest soil horizons was limited. Generally speaking, the current study provided an example on how spectral data can effectively be used for rapid and cost-effective prediction of SOC and TN at a national-scale from the upper to lower horizons of heterogeneous forest soils. Furthermore, the obtained outputs highlighted that VNIR–SWIR spectroscopy potential to be a suitable technique for quantifying and mapping forest organic layers (L, F and H) for the purposes of monitoring C:N. Nevertheless, the technique did not support the determination and mapping of C:N in the mineral horizons (A_1 and A_2) of the Czech Republic forested sites.

Detailed C:N information at different depths has the potential to set our understanding of soil functioning (Ben-Dor et al., 2008; Triantafilis et al., 2001). We thus suppose that the study of VNIR–SWIR spectroscopy in C:N assessment at different soil layers will be worthwhile and can further be used to assess soil quality and fertility (Lou et al., 2012; Zhou et al., 2021). It should be stated that there are still some external factors that noticeably affect the value and distribution of C:N. For instance, tree species and vegetation chemistry (Ollinger et al., 2002; Tajik et al., 2019) as well as climate regime and topographic factors such as slope and elevation leading to variation in C:N level (Ayoubi et al., 2012; Zhang et al., 2016). In addition, Kramer et al. (2012) and Wehr et al. (2020) specified that C:N depth patterns can be driven by soil minerals. Consequently, the capability of VNIR–SWIR spectra for C:N prediction and mapping will be affected, which need to be dealt with in future works.

5. Conclusions

This study explored the performance of laboratory VNIR–SWIR spectroscopy, SVMR machine learning technique and ordinary kriging to quantify SOC and TN and consequently to map the spatial distribution of the C:N in different soil layers of the forested sites of the Czech Republic. The conclusions of the study were as follows:

i) There was a large variation in the studied attributes in forest soil layers depending on the depth from which the samples were taken.
ii) A similar decreasing trend with depth was seen in average of the SOC and TN concentrations, except in the F layer. However, for C:N, the similar declining pattern by increasing depth was not observed. Layer L presented the highest C:N though the H layer showed the lowest C:N mean.
iii) Regardless of the depth, the average spectra shapes and patterns for all soil layers were generally similar, although layer H indicated the lowest albedo intensity and reflectance.
iv) The SOC and TN models for soil profile performed satisfactorily. Moreover, in terms of the prediction accuracy of the individual layers' models, layer F was the best-predicted forest soil layer for both SOC and TN.
v) C:N could be predicted in the soil profile and organic layers, particularly in layer F, but the developed models for the mineral layers poorly performed.
vi) Reflectance spectra could reasonably map the organic layers.
vii) A noticeable decrease in the map performances of layers A_1 and A_2 was observed, particularly in the areas with high C:N ($\geq$ 50), and it can be stated that VNIR–SWIR spectroscopy failed to show C:N variability in the mineral layers (A_1 and A_2).

As C:N is very dependent on forest tree species, topographic parameters and soil mineralogy, further hypothesis testing and

evaluating their effects on VNIR–SWIR predictive capability are planned.

Declaration of competing interest

The authors declare that they have no known competing financial interests or personal relationships that could have appeared to influence the work reported in this paper.

Acknowledgement

The authors like to thank the Central Institute for Supervising and Testing in Agriculture for providing the data. The authors also thank the financial support of the Czech Science Foundation (project No. 18-28126Y). The WORLDSOILS project by the European Space Agency developed within the EO Science for Society slice of the 5th Earth Observation Envelope Program is also acknowledged. The comments of Ran Pelta on preliminary methodology and the kind assistance of Luboš Borůvka and Lenka Pavlů for commenting on Czech soil classes and Karel Němeček for providing the detailed study area map are greatly appreciated.

References

Akselsson, C., Berg, B., Meentemeyer, V., & Westling, O. (2005). Carbon sequestration rates in organic layers of boreal and temperate forest soils — Sweden as a case study. *Global Ecology and Biogeography, 14*(1), 77–84.

Albrechtova, J., Seidl, Z., Aitkenhead-Peterson, J., Lhotakova, Z., Rock, Alexander, J. E., Malenovsky, Z., & McDowell, W. H. (2008). Spectral analysis of coniferous foliage and possible links to soil chemistry: Are spectral chlorophyll indices related to forest floor dissolved organic C and N? *Science of the Total Environment, 404*(2–3), 424–432.

Ayoubi, S., Mirbagheri, Z., & Mosaddeghi, M. R. (2020). Soil organic carbon physical fractions and aggregate stability influenced by land use in humid region of northern Iran. *International Agrophysics, 34*(3), 343–353.

Ayoubi, S., Mokhtari, P., Mosaddeghi, M. R., & Honarjoo, N. (2012). Soil aggregation and organic carbon as affected by topography and land use change in western Iran. *Soil & Tillage Research, 121*, 18–26.

Baciak, M., Warmiski, K., & Bes, A. (2015). The effect of selected gaseous air pollutants on woody plants. *Forest Research Papers, 76*, 401–409.

Barthes, B. G., Brunet, D., Ferrer, H., Chotte, J. L., & Feller, C. (2006). Determination of total carbon and nitrogen content in a range of tropical soils using near infrared spectroscopy: Influence of replication and sample grinding and drying. *Journal of Near Infrared Spectroscopy, 14*, 341–348.

Bellamy, P. H., Loveland, P. J., Bradley, R. I., Lark, R. M., & Kirk, G. J. D. (2005). Carbon losses from all soils across England and wales 1978-2003. *Nature, 437*, 245–248.

Bellon-Maurel, V., Fernandez-Ahumada, E., Palagos, B., Roger, J. M., & McBratney, A. B. (2010). Critical review of chemometric indicators commonly used for assessing the quality of the prediction of soil attributes by NIR spectroscopy. *TRAC Trends in Analytical Chemistry, 29*, 1073–1081.

Ben-Dor, E., & Banin, A. (1995). Near-infrared analysis as a rapid method to simultaneously evaluate several soil properties. *Soil Science Society of America Journal, 59*(2), 364–372.

Ben-Dor, E., Heller, D., & Chudnovsky, A. (2008). A novel method of classifying soil profiles in the field using optical means. *Soil Science Society of America Journal, 72*, 1113–1123.

Black, K., Creamer, R. E., Xenakis, G., & Cook, S. (2014). Improving forest soil carbon models using spatial data and geostatistical approaches. *Geoderma, 232*, 487–499.

Brahma, B., Pathak, K., Lal, R., Kurmi, B., Das, M., Nath, P. C., Nath, A. J., & Das, A. K. (2018). Ecosystem carbon sequestration through restoration of degraded lands in Northeast India. *Land Degradation & Development, 29*, 15–25.

Bremner, J. M., & Mulvaney, C. S. (1982). Nitrogen total 1. In *Methods of soil analysis. Part 2. Chemical and microbiological properties* (pp. 595–624). Madison, WI, USA: American Society of Agronomy, Soil Science Society of America, American Society of Agronomy.

Brunet, D., Barthes, B. G., Chotte, J. L., & Feller, C. (2007). Determination of carbon and nitrogen contents in alfisols, oxisols and ultisols from africa and Brazil using NIRS analysis: Effects of sample grinding and set heterogeneity. *Geoderma, 139*, 106–117.

Carre, F., Jeannee, N., Casalegno, S., Lemarchand, O., Reuter, H., & Montanarella, L. (2010). Mapping the CN ratio of the forest litters in Europe-Lessons for global digital soil mapping. In J. L. Boettinger, D. W. Howell, A. C. Moore, A. E. Hartemink, & S. Kienast-Brown (Eds.), *Digital soil mapping. Progress in soil science* (Vol. 2). Dordrecht, New York, NY, USA: Springer.

Chamberlain, P. M., Emmett, B. A., Scott, W. A., Black, H. I. J., Hornung, M., & Frogbrook, Z. L. (2010). No change in topsoil carbon levels of Great Britain, 1978–2007. *Biogeosciences Discussions, 7*, 2267–2311.

Chang, C. W., Laird, D. A., Mausbach, M. J., & Hurburgh, C., Jr. (2001). Near-infrared reflectance spectroscopy - principal component analysis of soil properties. *Soil Science Society of America Journal, 65*, 480–490.

Chen, D., Chang, N., Xiao, J., Zhou, Q., & Wu, W. (2019). Mapping dynamics of soil organic matter in croplands with MODIS data and machine learning algorithms. *Science of the Total Environment, 669*, 844–855.

Conforti, M., Castrignano, A., Robustelli, G., Scarciglia, F., Stelluti, M., & Buttafuoco, G. (2015). Laboratory-based Vis–NIR spectroscopy and partial least square regression with spatially correlated errors for predicting spatial variation of soil organic matter content. *Catena, 124*, 60–67.

Cook, R. (1977). Detection of influential observation in linear regression. *Technometrics, 19*, 15–18.

Cools, N., Vesterdal, L., Vos, B. D., Vanguelova, E., & Hansen, K. (2014). Tree species is the major factor explaining C:N ratios in European forest soils. *Forest Ecology and Management, 311*, 3–16.

Czech Statistical Office for Surveying. (2019). *Mapping and Cadastre*. URL: https://vdb.czso.cz.

Deluca, T. H., & Boisvenue, C. (2012). Boreal forest soil carbon: Distribution, function and modelling. *Forestry: An International Journal of Forestry Research, 85*(2), 161–184.

Dinakaran, J., Bidalia, A., Kumar, A., Hanief, M., Meena, A., & Rao, K. S. (2016). Near-infrared-spectroscopy for determination of carbon and nitrogen in Indian soils. *Communications in Soil Science and Plant Analysis, 47*(12), 1503–1516.

Dotto, A. C., Dalmolin, R. S. D., Caten, A. T., & Grunwald, S. (2018). A systematic study on the application of scatter-corrective and spectral-derivative preprocessing for multivariate prediction of soil organic carbon by Vis-NIR spectra. *Geoderma, 314*, 262–274.

England, J. R., & Viscarra Rossel, R. A. (2018). Proximal sensing for soil carbon accounting. *SOIL, 4*(2), 101–122.

Fiala, P., Reininger, D., Samek, T., Nemec, P., & Susil, A. (2013). *Pruzkum vyzivy lesa na uzemi Ceske Republiky 1996–2011*. Technical Report.

Gelaw, A. M., Singh, B. R., & Lal, R. (2013). Organic carbon and nitrogen associated with soil aggregates and particle sizes under different land uses in Tigray, Northern Ethiopia. *Land Degradation & Development, 26*, 7.

Ghebleh, M., Taghizadeh-Mehrjardi, R., Jafarzadeh, A. A., Triantafilis, J., & Lado, M. (2021). Using environmental variables and Fourier Transform Infrared Spectroscopy to predict soil organic carbon. *Catena, 202*, Article 105280.

Gholizadeh, A., Amin, M. S. M., Anuar, A. R., & Aimrun, W. (2011). Apparent electrical conductivity in correspondence to soil chemical properties and plant nutrients in soil. *Communications in Soil Science and Plant Analysis, 42*(12), 1447–1461.

Gholizadeh, A., Boruvka, L., Saberioon, M., & Vasat, R. (2013). Visible, near-infrared, and mid-infrared spectroscopy applications for soil assessment with emphasis on soil organic matter content and quality: State-of-the-art and key issues. *Applied Spectroscopy, 67*(12), 1349–1362.

Gholizadeh, A., Boruvka, L., Saberioon, M., & Vasat, R. (2016). A memory-based learning approach as compared to other data mining algorithms for the prediction of soil texture using diffuse reflectance spectra. *Remote Sensing, 8*(4), 341.

Gholizadeh, A., Viscarra Rossel, R. A., Saberioon, M., Boruvka, L., Kratina, J., & Pavlu, L. (2021). National-scale spectroscopic assessment of soil organic carbon in forests of the Czech Republic. *Geoderma, 385*, Article 114832.

Gholizadeh, A., Zizala, D., Saberioon, M., & Boruvka, L. (2018). Soil organic carbon and texture retrieving and mapping using proximal, airborne and Sentinel-2 spectral imaging. *Remote Sensing of Environment, 218*, 89–103.

Gibson, T., Chan, K., Sharma, G., & Shearman, R. (2002). *Soil carbon sequestration utilising recycled organics. Technical Report NSW Agriculture*.

Gitelson, A., Zur, Y., Chivkunova, O., & Merzlyak, M. (2002). Assessing carotenoid content in plant leaves with reflectance spectroscopy. *Photochemistry and Photobiology, 75*, 272–281.

Gomez, C., Gholizadeh, A., Boruvka, L., & Lagacherie, P. (2016). Using legacy data for correction of soil surface clay content predicted from VNIR/SWIR hyperspectral airborne images. *Geoderma, 276*, 84–92.

Guerrero, C., Wetterlind, J., Stenberg, B., Mouazen, A. M., Gabarron-Galeote, M. A., Ruiz-Sinoga, J. D., Zornoza, R., & Viscarra Rossel, R. A. (2016). Do we really need large spectral libraries for local scale soc assessment with NIR spectroscopy? *Soil & Tillage Research, 155*, 501–509.

Hastie, T., Tibshirani, R., & Friedman, J. (2009). *The elements of statistical learning: Data mining, Inference and Prediction*. Dordrecht, New York, NY, USA: Springer. Springer.

Heil, K., & Schmidhalter, U. (2021). An evaluation of different NIR-spectral pretreatments to derive the soil parameters C and N of a humus-clay-rich soil. *Sensors, 21*(4), 1423.

Holub, S. M., Lajtha, K., Spears, J. D. H., Toth, J. A., Crow, S. E., & Caldwell, B. A. (2005). Organic matter manipulations have little effect on gross and net nitrogen transformations in two temperate forest minerals in the USA and central Europe. *Forest Ecology and Management, 214*, 320–330.

Jenkinson, D., & Coleman, K. (2008). The turnover of organic carbon in subsoils. Part 2. Modelling carbon turnover. *European Journal of Soil Science, 59*(2), 400–413.

Jensen, J. (2007). *Remote sensing of the environment: An earth resource perspective* (Vol. 544). Prentice Education.

Jia, X., Chen, S., Yang, Y., Zhou, L., Yu, W., & Shi, Z. (2017). Organic carbon prediction in soil cores using VNIR and MIR techniques in an alpine landscape. *Scientific Reports, 7*, 2144.

Jiang, Q., Li, Q., Wang, X., Wu, Y., Yang, X., & Liu, F. (2017). Estimation of soil organic

carbon and total nitrogen in different soil layers using VNIR spectroscopy: Effects of spiking on model applicability. *Geoderma, 293*, 54–63.
Jia, S., Yang, X., Zhang, J., & Li, G. (2014). Quantitative analysis of soil nitrogen, organic carbon, available phosphorous, and available potassium using near-infrared spectroscopy combined with variable selection. *Soil Science, 179*(4), 211–219.
Ji, W., Li, S., Chen, S., Shi, Z., Viscarra Rossel, R., & Mouazen, A. M. (2016). Prediction of soil attributes using the Chinese soil spectral library and standardized spectra recorded at field conditions. *Soil & Tillage Research, 155*, 492–500.
Keesstra, S. D., Geissen, V., Mosse, K., Piiranen, S., Scudiero, E., Leistra, M., & Schaik, van L. (2012). Soil as a filter for groundwater quality. *Current Opinion in Environmental Sustainability, 4*, 507–516.
Kennard, R. W., & Stone, L. A. (1969). Computer aided design of experiments. *Technometrics, 11*, 137–148.
Kim, M. G. (2017). A cautionary note on the use of Cook's distance. *Communications for Statistical Applications and Methods, 24*, 317–324.
Knadel, M., Deng, F., Thomsen, M. A., & Greve, M. H. (2012). Development of a Danish national Vis-NIR soil spectral library for soil organic carbon determination. In B. Minasny, B. P. Malone, & A. B. McBratney (Eds.), *Digital soil assessments and beyond. Proceedings of the 5th global workshop on digital soil mapping 2012*. CRC Press.
Kooistra, L., Wanders, J., Epema, G., Leuven, R., Wehrens, R., & Buydens, L. (2003). The potential of field spectroscopy for the assessment of sediment properties in river floodplains. *Analytica Chimica Acta, 484*, 189–200.
Kovacevic, M., Bajat, B., Trivic, B., & Pavlovic, R. (2009). Geological units classification of multispectral images by using support vector machines. In Y. K. Badr, S. Caballe, F. Xhafa, A. Abraham, & B. Gros (Eds.), *International conference on intelligent networking and collaborative systems* (pp. 267–272). New York, NY, USA: IEEE.
Kramer, M. G., Lajtha, K., & Aufdenkampe, A. K. (2017). Depth trends of soil organic matter C:N and ^{15}N natural abundance controlled by association with minerals. *Biogeochemistry, 136*(4), 237–248.
Kramer, M. G., Sanderman, J., Chadwick, O. A., Chorover, J., & Vitousek, P. M. (2012). Long-term carbon storage through retention of dissolved aromatic acids by reactive particles in soil. *Global Change Biology, 18*(8), 2594–2605.
Krull, E. S., & Skjemstad, J. O. (2003). d 13 C and d 15 N profiles in 14 C-dated Oxisol and Vertisols as a function of soil chemistry and mineralogy. *Geoderma, 112*(1), 1–29.
Kuang, B., & Mouazen, A. M. (2011). Calibration of visible and near infrared spectroscopy for soil analysis at the field scale on three European farms. *European Journal of Soil Science, 62*, 629–636.
Kukal, D., & Bawa, S. S. (2014). Soil organic carbon stock and fraction in relation to land use and soil depth in the degraded shiwaliks hills of lower Himalayas. *Land Degradation & Development, 25*, 407–416.
Lal, R. (2008). Carbon sequestration. *Philosophical Transactions of the Royal Society of London - B, 363*, 815–830.
Lal, R. (2017). *Carbon management, technologies, and trends in Mediterranean ecosystems* (Vol. 15, pp. 1–11). Dordrecht, New York, NY, USA: Springer.
Li, Q., Fang, H. Y., Sun, L. Y., & Cai, Q. G. (2014). Use the CS technique to study the effect of soil redistribution on soil organic carbon and total nitrogen stocks in an agricultural catchment of Northeast China. *Land Degradation & Development, 25*, 350–359.
Lin, L. I. (1989). A concordance correlation coefficient to evaluate reproducibility. *Biometrics, 45*, 255–268.
Lou, Y., Xu, M., Chen, X., He, X., & Zhao, K. (2012). Stratification of soil organic C, N and C:N ratio as affected by conservation tillage in two maize fields of China. *Catena, 95*, 124–130.
Martens, H., & Naes, T. (1992). *Multivariate calibration*. New York, USA: John Wiley Sons.
Mouazen, A. M., Baerdemaeker, J. D., & Ramon, H. (2005). Towards development of on-line soil moisture content sensor using a fibre-type NIR spectrophotometer. *Soil & Tillage Research, 80*, 171–183.
Munoz-Rojas, M., Jordan, A., Zavala, L. M., Rosa, D., Abd-Elmabod, S. K., & Anaya-Romero, M. (2015). Impact of land use and land cover changes on organic carbon stocks in Mediterranean soils (1956–2007). *Land Degradation & Development, 25*, 168–179.
Murphy, B. W. (2014). *Soil organic matter and soil function – review of the literature and underlying data*. Canberra, Australia: Department of Environment.
Mutuo, P. K., Shepherd, K. D., Albrecht, A., & Cadisch, G. (2006). Prediction of carbon mineralization rates from different soil physical fractions using diffuse reflectance spectroscopy. *Soil Biology and Biochemistry, 38*, 1658–1664.
Naimi, S., Ayoubi, S., Raimo, A. D., & Dematte, J. A. (2022). Quantification of some intrinsic soil properties using proximal sensing in arid lands: Application of Vis-NIR, MIR, and pXRF spectroscopy. *Geoderma Regional, 28*, Article e00484.
Nolan, T., Troy, S. M., Healy, M. G., Kwapinski, W., Leahy, J. J., & Lawlor, P. G. (2011). Characterization of compost produced from separated pig manure and a variety of bulking agents at low initial C/N ratios. *Bioresource Technology, 102*(14), 7131–7138.
Ollinger, S. V., Smith, M. L., Martin, M. E., Hallett, R. A., Goodale, C. L., & Aber, J. D. (2002). Regional variation in foliar chemistry and N cycling among forests of diverse history and composition. *Ecology, 83*, 339–355.
Peltre, C., Thuries, L., Barthes, B. G., Brunet, D., Morvan, T., Nicolardot, B., Parnaudeau, V., & Houot, S. (2011). Near infrared reflectance spectroscopy: A tool to characterize the composition of different types of exogenous organic matter and their behaviour in soil. *Soil Biology and Biochemistry, 43*(1), 197–205.
Radocaj, D., Jurisic, M., & Antonic, O. (2021). Determination of soil C:N suitability zones for organic farming using an unsupervised classification in eastern Croatia. *Ecological Indicators, 123*, Article 107382.
Savitzky, A., & Golay, M. (1964). Smoothing and differentiation of data by simplified least squares procedures. *Analytical Chemistry, 36*, 1627–1639.
Shang, Z. H., Cao, J., Guo, R., Henkin, Z., Ding, L., Long, R., & Deng, B. (2014). Effect of enclosure on soil carbon nitrogen and phosphorus of alpine desert rangeland. *Land Degradation & Development, 28*, 1166–1177.
Sherman, D. M., & Waite, T. D. (1985). Electronic spectra of Fe^{3+} oxides and oxyhydroxides in the near infrared to ultraviolet. *American Mineralogist, 70*, 1262–1269.
Shi, T., Wang, J., Chen, Y., & Wu, G. (2016). Improving the prediction of arsenic contents in agricultural soils by combining the reflectance spectroscopy of soils and rice plants. *International Journal of Applied Earth Observation and Geoinformation, 52*, 95–103.
Song, Y., Li, F., Yang, Z., Ayoko, G. A., Frost, R. L., & Ji, J. (2012). Diffuse reflectance spectroscopy for monitoring potentially toxic elements in the agricultural soils of Changjiang River Delta, China. *Applied Clay Science, 64*, 75–83.
Sorenson, P. T., Quideau, S. A., Rivard, B., & Dyck, M. (2020). Distribution mapping of soil profile carbon and nitrogen with laboratory imaging spectroscopy. *Geoderma, 359*, Article 113982.
Sparks, D. (1996). *Methods of soil analysis. Part 3. Chemical Methods*. Madison, WI, USA: Soil Science Society of America, American Society of Agronomy. Madison, WI, USA.
Stevens, A., Nocita, M., Toth, G., Montanarella, L., & van Wesemael, B. (2013). Prediction of soil organic carbon at the European scale by visible and near infrared reflectance spectroscopy. *PLoS One, 8*, 1–13.
Tajik, S., Ayoubi, S., Khajehali, J., & Shataee, S. (2019). Effects of tree species composition on soil properties and invertebrates in a deciduous forest. *Arabian Journal of Geosciences, 12*(11), 368.
Telles, E., de Camargo, P. B., Martinelli, L. A., Trumbore, S. E., da Costa, E. S., Santos, J., Higuchi, N., & Oliveira, R. C., Jr. (2003). Influence of soil texture on carbon dynamics and storage potential in tropical forest soils of Amazonia. *Global Biogeochemical Cycles, 17*(2), 1040.
Triantafilis, J., Ward, W., Odeh, I., & McBratney, A. B. (2001). Creation and interpolation of continuous soil layer classes in the lower Namoi valley. *Soil Science Society of America Journal, 65*, 403–413.
Ugawa, S., Takahashi, M., Morisada, K., Takeuchi, M., Yoshinaga, S., Araki, M., Tanaka, N., Ikeda, S., Matsuura, Y., Miura, S., Ishizuka, S., Kobayashi, M., Inagaki, M., Imaya, A., Nanko, K., Hashimoto, S., Aizawa, S., Hirai, K., Okamoto, T., Mizoguchi, T., Torii, A., Sakai, H., Ohnuki, Y., & Kaneko, S. (2012). Carbon stocks of dead wood, litter, and soil in the forest sector of Japan: General description of the national forest soil carbon inventory. *Bulletin FFPRI, 11*, 207–221.
Vanguelova, E. I., Bonifacio, E., Vos, B. D., Hoosbeek, M. R., Berger, T. W., Vesterdal, L., Armolaitis, K., Celi, L., Dinca, L., Kjnaas, O. J., Pavlenda, P., Pumpanen, J., Puttsepp, Reidy, B., Simoncic, P., Tobin, B., & Zhiyanski, M. (2016). Sources of errors and uncertainties in the assessment of forest soil carbon stocks at different scales review and recommendations. *Environmental Monitoring and Assessment, 188*, 630.
Viscarra Rossel, R. A., & Behrens, T. (2010). Using data mining to model and interpret soil diffuse reflectance spectra. *Geoderma, 158*, 46–54.
Viscarra Rossel, R. A., Brus, D., Lobsey, C., Shi, Z., & McLachlan, G. (2016). Baseline estimates of soil organic carbon by proximal sensing: Comparing design-based, model-assisted and model-based inference. *Geoderma, 265*, 152–163.
Viscarra Rossel, R. A., & Hicks, W. S. (2015). Soil organic carbon and its fractions estimated by visible near infrared transfer functions. *European Journal of Soil Science, 66*, 438–450.
Viscarra Rossel, R. A., Lobsey, C. R., Sharman, C., Flick, P., & McLachlan, G. (2017). Novel soil profile sensing to monitor organic C stocks and condition. *Environmental Science & Technology, 51*(10), 5630–5641.
Vohland, M., Besold, J., Hill, J., & Frund, H. C. (2011). Comparing different multivariate calibration methods for the determination of soil organic carbon pools with visible to near infrared spectroscopy. *Geoderma, 166*, 198–205.
Vries, W. D., Reinds, G. J., Gundersen, P., & Sterba, H. (2006). The impact of nitrogen deposition on carbon sequestration in European forests and forest soils. *Global Ecology and Biogeography, 12*(7), 1151–1173.
Wang, Y., Jiang, J., Niu, Z., Li, Y., Li, C., & Feng, W. (2019). Responses of soil organic and inorganic carbon vary at different soil depths after long-term agricultural cultivation in Northwest China. *Land Degradation & Development, 30*, 1229–1242.
Wehr, J. B., Lewis, T., Dalal, R. C., Menzies, N. W., Verstraten, L., Swift, S., Bryant, P., Tindale, N., & Smith, T. E. (2020). Soil carbon and nitrogen pools, their depth distribution and stocks following plantation establishment in south east Queensland, Australia. *Forest Ecology and Management, 457*, Article 117708.
Wilding, L. (1985). Spatial variability: Its documentation, accomodation and implication to soil surveys. In J. P. Bouma, & D. R. Nielsen (Eds.), *Workshop on soil spatial variability*.
Xie, H., Yang, X., Drury, C., Yang, J., & Zhang, X. (2011). Predicting soil organic carbon and total nitrogen using mid-and near-infrared spectra for Brookston clay loam soil in Southwestern Ontario, Canada. *Canadian Journal of Soil Science, 91*, 53–63.
Xu, Y., Li, Y., Li, H., Wang, L., Liao, X., Wang, J., & Kong, C. (2018). Effects of topography and soil properties on soil selenium distribution and bioavailability (phosphate extraction): A case study in yongjia county, China. *Science of the Total Environment, 633*, 240–248.

Zanella, A., Ponge, J. F., Jabiol, B., Sartori, G., Kolb, E., Gobat, J. M., Bayon, R. C. L., Aubert, M., Waal, R. D., Delft, B. V., Vacca, A., Serra, G., Chersich, S., Andreetta, A., Cools, N., Englisch, M., Hager, H., Katzensteiner, K., Brthes, A., Nicola, C. D., Testi, A., Bernier, N., Graefe, U., Juilleret, J., Banas, D., Garlato, A., Obber, S., Galvan, P., Zampedri, R., Frizzera, L., Tomasi, M., Menardi, R., Fontanella, F., Filoso, C., Dibona, R., Bolzonella, C., Pizzeghello, D., Carletti, P., Langohr, R., Cattaneo, D., Nardi, S., Nicolini, G., & Viola, F. (2017). Humusica 1, article 4: Terrestrial humus systems and forms Specific terms and diagnostic horizons. *Applied Soil Ecology, 122*, 56–74.

Zhang, W., Ricketts, T. H., Kremenc, C., Carneyd, K., & Swintona, S. M. (2007). Ecosystem services and dis-services to agriculture. *Ecological Economy, 64*, 253–260.

Zhang, S., Yan, L., Huang, J., Mu, L., Huang, Y., Zhang, X., & Sun, Y. (2016). Spatial heterogeneity of soil C:N ratio in a Mollisol watershed of northeast China. *Land Degradation & Development, 27*, 295–304.

Zhao, Z., Wei, X., Wang, X., Ma, T., Huang, L., Gao, H., Fan, J., Li, X., & Jia, X. (2019). Concentration and mineralization of organic carbon in forest soils along a climatic gradient. *Forest Ecology and Management, 432*, 246–255.

Zhou, T., Geng, Y., Ji, C., Xu, X., Wang, H., Pan, J., Bumberger, J., Haase, D., & Lausch, A. (2021). Prediction of soil organic carbon and the C:N ratio on a national scale using machine learning and satellite data: A comparison between sentinel-2, sentinel-3 and landsat-8 images. *Science of the Total Environment, 755*(2), Article 142661.